Determining Optimal Zone Radius of Zone Routing Protocol Based on Deep Recurrent Neural Networks in the Next Generation Wireless Backhaul Networks

Fadli Sirait [a, b,*], Mohd Taufik Bin Jusoh [b], Kaharudin Dimyati [c], Muhammad Faiz Bin Md Din [b]

[a] Electrical Engineering, Universitas Mercu Buana, Jakarta, 11650, Indonesia
[b] Electrical and Electronics Engineering, National Defence University of Malaysia, Kuala Lumpur, 57000, Malaysia
[c] Electrical Engineering, University of Malaya, Kuala Lumpur, 50603, Malaysia
Corresponding author: *fadli.sirait@mercubuana.ac.id

Abstract—**Next-generation wireless networks are becoming more popular and rely on reliable backhaul networks to work properly. Wireless backhaul networks also adopt various innovative technologies to improve capacity and provide more flexible deployments to meet networks' high-quality requirements. One of the essential innovations to maintain the wireless backhaul performance is combining the existing routing protocol technology and the deep learning concept. The concept of deep learning is gaining traction as a powerful way to add intelligence to wireless networks with complex topologies and radio environments. This is because conventional routing protocols do not learn from their previous experiences with various network anomalies. This paper proposed a predictive model of zone radius value using the deep recurrent neural network variant, namely the long short-term memory recurrent neural network (LSTM-RNN) algorithm. Determination of zone radius value conducted by measuring the whole of nodes routing zone using various network performance as input parameters such as** Routing **Overhead, Energy Consumption, Throughput, and User Usage. Performance measurements such as mean square error (MSE), error distribution histogram, training state, regression, correlation, and time series response are gauged and compared for static and mobile node environments. Results showed that the proposed algorithm can accurately predict zone radius for both environments. However, the accuracy of the proposed algorithm is higher when implemented in a static node environment.**

Keywords— **Zone radius; wmn; routing protocol; zrp; lstm-rnn.**

I. Introduction

There is a tremendous surge in data communication due to the increase in mobile devices interconnection and infrastructures for wired/wireless communication networks [1]. It impacts the increasing use of unlicensed spectrum in the next-generation wireless network communication systems [2]. The implementation of wireless backhaul networks is urgently needed, particularly in the area that is hard to access or develop network infrastructure at all sites [3]. One of the most potential network infrastructures that can be used as wireless backhaul is a wireless mesh network (WMN), which implements multi-hop connectivity by less installing cables that impact the cost and easier deployment in the problematic area[4].
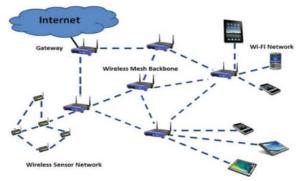

Fig. 1 Architecture of Infrastructure/Backbone WMN

Routing protocol assures the stability of communication in WMN, where the selection of proper routing protocol is one of the main issues to reach the required high performance of

network connectivity services in neighboring community networks, corporate networks, MAN, systems of transportation, buildings with automatic control, systems of medicine and health or surveillance [5]. Several factors are considered when designing an effective routing protocol, including rapidly changing connectivity, network partition, greater error rates, collision interference, bandwidth, and power constraints [6].

The development of routing protocol in the dynamic wireless network environment that can discover and maintain the routes efficiently refers to the classification of routing protocols described in Table 1.

TABLE I
CLASSIFICATION OF ROUTING PROTOCOL

Issues	Proactive	Reactive	Hybrid
Main Features	At all times, keep routing information on all nodes in the network.	Maintain routing information for only those nodes that are required at any time given time.	Combining the features of Proactive and reactive, where proactive for short distances and reactive for long distances
Benefit	Low route setup	Low routing overhead	No route setup required
Drawback	High routing overhead	Larger route setup	More complex
Examples	DSDV[7], OLSR[8], STAR[9], WRP[10]	AODV[8], DSR [9]	ZRP[11], TORA[12]

In Table 1, ZRP is the most popular hybrid routing protocol in WMN by implementing zone-based routing protocols and utilizing the benefit of both reactive and proactive protocol mechanisms [13].
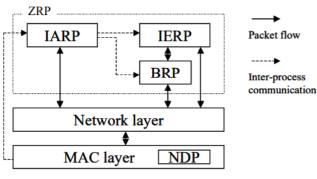

Fig. 2 Architecture of ZRP

ZRP as a routing protocol is considered one of the potential methods to implement in the next-generation wireless network to maintain the network's link stability. The use of ZRP is expected to reduce the control overhead due to the proactive routing protocol process and cut down the latency as an impact of reactive routing protocol in the routing discovery process [14]. There is four subprotocol in ZRP, including IntrA-zone Routing Protocol (IARP) [15] as a locally proactive routing protocol approach based on periodic maintenance within the routing zone. The next is IntEr-zone Routing Protocol (IERP) [16], a globally reactive routing protocol component that provides increased route discovery and maintenance based on local connection. Furthermore, the

Bordercast Resolution Protocol (BRP) is used as the bordercast package delivery service to find the new route needed by the source node to reduce excessive demand. Neighbor Discovery Protocol (NDP) is a sub-protocol provided by the MAC layer to detect whether there exist new neighbor nodes and/or link failures in the network. At regular intervals, NDP sends out "HELLO" beacons. The neighbor table is updated when a beacon is received. Neighbors who have not gotten a beacon in a certain time are removed from the table. If the MAC layer does not include an NDP, the functionality must be provided by IARP [17]. The performance of ZRP is influenced by a property called zone radius, which represents the number of hops from a source node to the zone's boundaries [13]. Determining the optimal value of zone radius is one of the main issues in reaching the efficient ZRP cost process[18].

Some researchers are researching how to efficiently and effectively optimize network traffic control by optimizing the zone radius parameter in the zone routing protocol [6] [19]. However, using computational machine learning methods appears as a key challenge due to conventional routing protocols' inability to learn from their prior network abnormality experiences [20]. Naser et al. [21] propose the employment of two deep RNN variants: long short-term memory recurrent neural network (LSTM-RNN) and gated recurrent unit (GRU) to predict link quality (LQ) in wireless community network (WCN) with high accuracy. Jaffry and Hasan [22] have designed an LSTM-based cellular traffic prediction model by comparing the LSTM-based prediction with the baseline ARIMA (Autoregressive integrated moving average) model and vanilla feed-forward neural network (FFNN). The final results show that LSTM models as the most effective method to predict future cellular traffic.

Nugraha et al. [23] propose a hybrid Convolutional Neural Network-Long Short-Term Memory (CNN-LSTM) model for detecting slow DDoS attacks in SDN-based networks, with performance metrics above 99%. Mei et al. [24] studied real-time mobile bandwidth prediction in various scenarios by developing LSTM-RNN models to catch the complex temporal structures in mobile bandwidth traces for accurate prediction. The final results of the research showed that LSTM achieves significant accuracy improvements over state-of-the-art prediction algorithms.

In this paper, the LSTM-RNN as a variant of the deep RNN was proposed to determine the optimal zone radius of ZRP implemented in WMN to improve protocol performance and reduce control traffic. The LSTM-RNN algorithm exploited parameters collected from the network model developed to predict the best value of zone radius. Parameters collected from the networks model are used as a dataset in the experiments performed, including Routing Overhead, Energy Consumption, Throughput, and User Usage. The data set was split into 500 for data training and 100 for data testing. The simulation results show that the accuracy of the zone radius prediction model is significantly based on the value of MSE, drawing error distribution histogram, training state, regression, autocorrelation, and time series response. The rest of this paper is organized as follows: the Design and development of the proposed model are described in section II, in section III, the Experiment Results and Discussion are

described, and the conclusion of this paper is described in section IV.

II. MATERIALS AND METHOD

In this research, the ZRP is optimized by applying computational methods of deep learning using LSTM-RNN to determine the optimal zone radius. This approach is expected to reduce the amount of traffic control due to the growing use of data traffic in the networks. Firstly, the data packet is transmitted to the receiver node by the sender node. In this process, the sender node used specifier input of zone radius technique. The source node used an IARP routing table to determine whether or not the receiver node's destination was within the zone. If the destination is out of the zone, IERP will be used to find the receiver node within the zone. The request is border-cast by the source node to peripheral nodes.

Once they found the required receiver nodes, the sender node sent a route request to locate the desired destination of receiver nodes in its routing zone. Then, the receiver node sends the feedback and routes the reply to the sender node. The route reply provides available multiple paths.
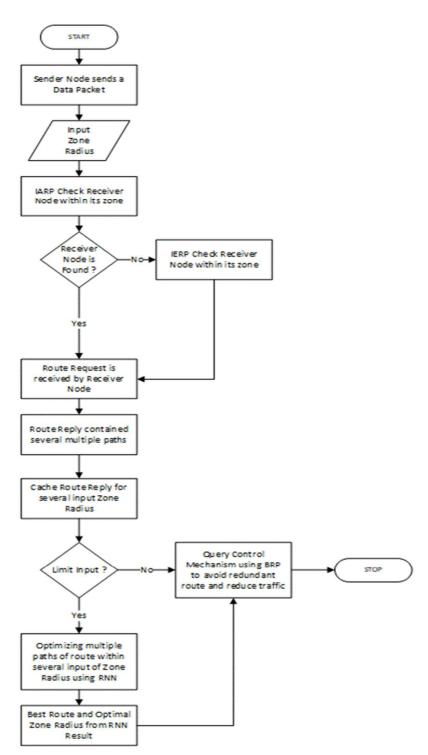

Fig. 3 Proposed Model

Before the source node sends data according to some of the reply routes provided, the results are cached in the cache and simulated for the next input zone radius. The route reply obtained is done using the BRP query control mechanism to avoid redundant routes. If there is a redundant route, then the route is dismissed from the cache and continued with the determination of the route with the next input of Zone Radius.

When all route replies containing multiple route paths with several radius zones are stored in the cache, then deep learning techniques with LSTM-RNN are optimized. The next step is selecting the best route using LSTM-RNN by comparing the fitness of the input zone radius value that impacts the value of Routing Overhead (RO), Energy Consumption, Achievable Throughput, and user usage. Once the optimization results are obtained by doing this process, it resumes back to the stage of determining the query control mechanism using BRP, and the results obtained can reduce traffic usage in the network.

A. Recurrent Neural Network

RNNs are neural networks organized into iterative layers forming sequential data that apply to time series [25]. In recurrent neural networks, the process for making the current prediction is based on the main idea of the use of input data and also the previous outputs. Therefore, neural networks can build by passing values forward in time. For each time step t, the first procedure calculates the state st from the input (x_t) and the previous state (s_{t-1}), each multiplied by the parameters U and W and then processed with the tanh activation function.

$$s_t = \tanh(U \cdot x_t + W \cdot s_{t-1}) \qquad (1)$$

From s_t, then the output o_t is calculated by multiplying it by the parameter V and passing it to the $softmax$ activation function:

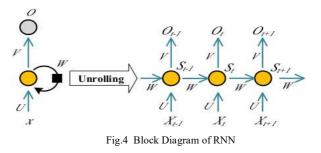$$o_t = softmax(V \cdot s_t) \qquad (2)$$

Since the parameters U, V, and W (especially U and W) contain the calculations of the previous time step, to calculate the gradient in the time step t, derivatives in time steps *t-1, t-2, t-3* have to calculate, and so on until the starting point ($t = 1$). Backpropagation Through time is a traditional method that computes sufficient gradients for training a particular RNN model [21]. The expression of the gradients demonstrates as follows [26]:

$$\frac{\partial E_t}{\partial \theta} = \sum_{1 < t \ll T} \frac{\partial E_t}{\partial \theta} \qquad (3)$$

However, there are problems in training RNNs for modeling long-term dependencies due to the vanishing/explosion problem of the gradients of the utilized cost function, as noticed in eq. (1) [27].

$$\frac{\partial E_t}{\partial \theta} = \sum_{1 < t \ll T} \frac{\partial E_t}{\partial h_t} \frac{\partial h_t}{\partial h_k} \frac{\partial^+ h_k}{\partial \theta} \qquad (4)$$

To solve this problem, several review papers proposed an approach: Long short-term memory (LSTM) as one of the most popular RNN units used for sequence modeling tasks [28].

Fig.4 Block Diagram of RNN

B. LSTM

To deal with the issues of training RNNs that can learn short and long-term dependencies, LSTM is being used [28]. The emergence of long-term dependency in RNNs can be prevented by the implementation of LSTM due to their memory blocks being connected across layers [21]. In LSTM, a block has gates to calculate its state and the predicted output. The LSTM block has three gates: a forget gate, an input gate, and an output gate. The expression for LSTM operation is as follows:

$$i_t = \sigma(W x_i X_t + W_{hi} h_{t-1} + W_{ci} c_{t-1} + b_i) \qquad (5)$$

$$i_t = \sigma(W x_i X_t + W_{hi} h_{t-1} + W_{ci} c_{t-1} + b_i) \qquad (6)$$

$$f_t = \sigma\big(W x f X_t + W_{hf} h_{t-1} + W_{cf} c_{t-1} + b_f\big) \qquad (7)$$

$$c_t = f_1 c_{t-1} + i_t \tanh(W_{xc} X_t + W_{hc} h_{t-1} + b_c) \qquad (8)$$

$$o_t = \sigma(W_{xo} X_t + W_{ho} h_{t-1} + b_o) \qquad (9)$$

$$h_t = o_t tanh(c_t) \qquad (10)$$

Note: W is referred to the weight of the corresponding hidden neural in the LSTM block.

III. Results and Discussion

An experiment was conducted to validate the test prediction accuracy of zone radius for conventional ZRP and ZRP with an LSTM-RNN algorithm that was implemented in two types of environments, such as static and mobile node environments. Furthermore, both algorithms were compared to observe their performance of them. The bandwidth capacity used in the network was 300 Mbps meeting the minimum requirement of 5G network bandwidth capacity [29], and the zone radius value varies from 2-6 hops [30]. Experiment results showed that in static node, 72% of zone radius value for LSTM-RNN algorithm is lower than the value of zone radius for conventional ZRP. Meanwhile, in the mobile node, 54% of the zone radius value for the LSTM-RNN algorithm is lower than the value of zone radius for conventional ZRP. The changes in zone radius value were influenced by control messages related to the reactive routing approach (Route REQest (RREQ), Route ERROR (RERROR), and route reply packets of IARP) and control messages related to the table-driven routing approach (IARP) [30].

When the zone radius value increases, the area of proactive-routing services in the network also increases and reduces the reactive-routing services, and conversely, when decreasing the zone radius value [18]. The experiment results show that in the static node environment, the reactive routing process was dominant when implementing LSTM-RNN instead of the proactive routing process and vice versa when implementing conventional ZRP. Meanwhile, in the mobile

node environment, the Reactive routing process is also dominant when implementing LSTM-RNN instead of proactive routing process, and vice versa when implementing conventional ZRP. Nevertheless, there was a decreasing percentage of zone radius for the mobile node environment in comparison with the static node environment when implemented LSTM-RNN and vice versa when implemented conventional ZRP.

A. Performance Evaluation of LSTM-RNN

Performance evaluation of LSTM-RNN is necessary to determine the range of errors based on the MSE (Minimum Square Error) obtained during the iteration process (epoch) from the beginning to the optimum value of MSE [31]. The mean square error (MSE) in LSTM is considered the lost function [21], it is always non-negative, and a smaller value of MSE represents to smaller estimation error [32].

The formula of MSE can be expressed as follows:

$$MSE = \frac{1}{N}\sum_{i=1}^{N}(R_i^{actual} - R_i^{predicted})^2 \qquad (11)$$

Where, N is the observation number, R_i^{actual} is the value of the actual zone radius, and $R_i^{predicted}$ is the value of the predicted zone radius.
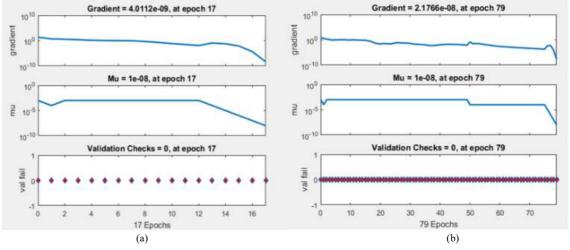

Fig. 5 MSE value for (a) Static Node Environment, (b) Mobile Node Environment

Fig. 5 demonstrates the MSE value for static (a) and mobile node environment (b). The best value of training process in LSTM-RNN for static node environment reach in 17th epoch, with the value of MSE is 1,7968e-18, and 79th epoch for mobile node environment with the value of MSE is 5,154e-18. From the results, the implementation of LSTM-RNN for the Static node environment has a lower MSE value than the implementation for the mobile node environment. A static node environment is better than a mobile node environment implementation. Overall, the implementation of LSTM-RNN for a static node environment has a smaller value of MSE than LSTM-RNN for the mobile node, and it represents the smaller

MSE value has better accuracy in terms of zone radius prediction. Nevertheless, both MSE value for both environments is acceptable.

B. Training State

The results of LSTM-RNN train state were conducted to determine the value of gradient, Mu, and validation checks. Fig.6 shows the results of LSTM-RNN train state obtained during the process for static (a) and mobile node environment (b). The gradient function is the most common method used for updating the weights of the neural networks [33], so it can allow the LSTM-RNN model to conduct the training process.
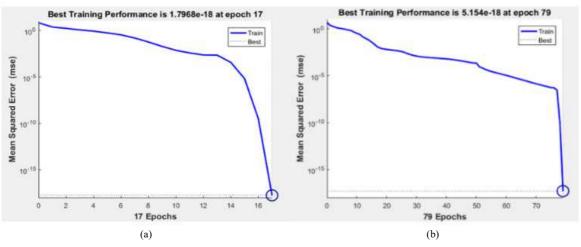

Fig. 6 Training State: (a) Static Node Environment, (b) Mobile Node Environment

The objective of adjusting weights and tendencies is to obtain the lowest value of error (loss function), which is the lower error that gets during the process, the better performance of LSTM-RNN reaches [32]. The number of epochs throughout the process affects to the gradient problem [34]. Consequently, it is necessary to conduct a backpropagation to minimize the pain of the vanishing gradient [35]. However, the backpropagation method also impacts the presence of exploding gradient [27], [36].

In Fig. 6, there is evidence that the gradient is locally decreasing as a function of the epoch; in other words, the error should decrease as the number of iterations increases [37]. The value of gradient during the LSTM-RNN process for the static node environment is $4.0112e^{-9}$ at epoch 17th, and $2.1766e^{-8}$ at epoch 79th for mobile node environment.

From those results, it is known that the value of the gradient of LSTM-RNN for static node is lower than the value of the gradient for mobile node environment. The duration needed to reach the best gradient value in LSTM-RNN for mobile node environment is more elongated than the period for static node environment. It is demonstrated that the gradient value for the static node environment is better than the mobile node environment.

Mu value is used to control the weight of the neuron update process (backpropagation) during the training process; Mu is commonly termed momentum [38]. From the experiment results, it can be seen that the value of Mu for both static and mobile node environments is $1e^{-8}$ reached at 17th epoch for static node and 79th epoch for mobile node environment.

When the validation error does not improve for a number of consecutive epochs, the validation check serves as an early warning system, stopping training and checking the error on the validation set [39]. From the experiment results, the value of the validation checks for both environments is 0; it represented the number of error repetitions is 0, and stopped at 17th and 79th epoch for static and mobile node environments, respectively.

C. Error Histogram (Histogram Deviation)

The results of the error histogram on simulation were conducted to determine the range of deviation between the target and predicted value during the process. These error numbers can be negative since they represent how anticipated values depart from target values.
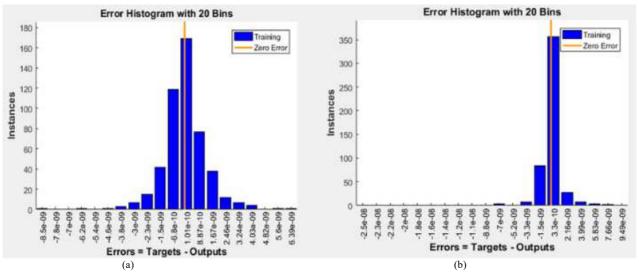

Fig. 7 Error Histogram: (a) Static Node Environment, (b) Mobile Node Environment

In Fig. 7, there are 20 blue vertical bars (bins), with the red vertical line representing zero error tolerance limit. Zero error line corresponds to the error axis's zero error value (i.e.-axis). The number of samples (instances) of training data is represented on the Y-axis; meanwhile, 20 blue vertical bars on the X-axis represent the histogram deviation value (error). Moreover, the height of the bar in the bar plot means how many data points are near the bin value. From Fig. 7, it can be seen that for static node environment (a), zero error point falls the center $1.01e^{-10}$. Meanwhile, for mobile node environment (b) is $3.3e^{-10}$. From both static and mobile node environments, the value of the error histogram for static node environment is more significant than the value of the error histogram for the mobile node environment. Nevertheless, both of the results are acceptable and demonstrated that the value of error for both environments was very small

D. Regression

Fig. 8 demonstrates the results of the fit value of the regression between target value (t) and predicted value (y) obtained during the training process for static node (a) and mobile node environment (b). Due to the value of the correlation coefficient (R) being 1 for both environments, then the linear relationship is a perfect positive correlation (close relationship) [40]. Therefore, the fit value between the target and the predicted value is no difference, indicated by the dotted line under the R-value of 1 (linearly dependent). If the value of R is close to 0, it is indicated that the model fails in making a prediction. Furthermore, the absence of the difference between the target and the predicted value also indicates that the training process results are doing well, and results are acceptable.
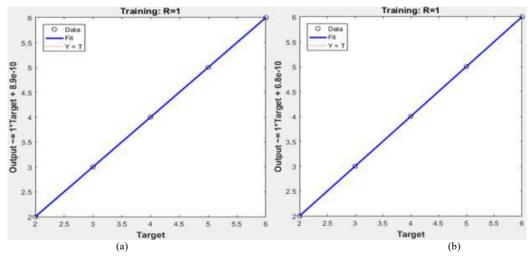
Fig. 8 Correlation Regression: (a) Static Node Environment, (b) Mobile Node Environment

The results show that the correlation regression value for both environments has the same value (R=1). Nevertheless, the regression value for a static node is higher than for a mobile node environment. This circumstance demonstrated a strong regression between target and predicted value for static and mobile node environments. The absence of a difference between target and predicted value in both environments indicated that the training process results are doing well, and the results are acceptable.

E. Time Series Response

The use of time series response is described as:
- To obtain the value of response comparison between time-series target values (t) and time-series output values
- To obtain the value of error comparison between time-series target values (t) and time-series output values.
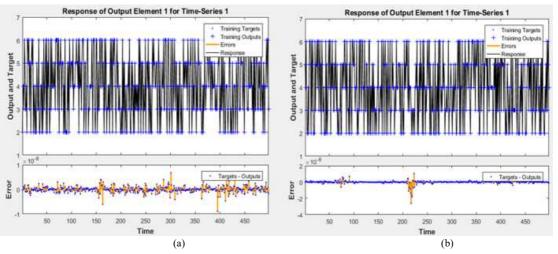

Fig. 9 Time Series Response: (a) Static Node Environment, (b) Mobile Node Environment

Fig. 9 demonstrates the comparison between target time series values and output time series values for static node (a) in the error range from -0.8 to 0.8, representing the distribution of error along the time series axis is dominant close to zero (zero error). In other words, the value of error in time series during the process is minimal. Meanwhile, for mobile node environment (b), the range of error from -3.2 to 1.6, and the distribution of error along the time series axis is also dominant close to zero (zero error). From that time-series response for static and mobile node environments, it can be seen that the distribution of error between the value of the target and the value of output for the static node environment is more significant than in comparison with the mobile node environment. The response of both target time series value and output time series value shows that the range of

distribution time series is 2 to 6, representing the results of the maximum zone radius value obtained during the process for both environments.

F. Autocorrelation

Autocorrelation is used to discover the relationship or correlation between the target and predicted value. Autocorrelation is described in terms of how the correlation value is compared to the lag, which is the dependence of the target value on the predicted value of the time-series data distribution at certain time intervals. There should only be one nonzero value of the autocorrelation function in the perfect prediction model, and this nonzero value should occur at zero lag. [41].
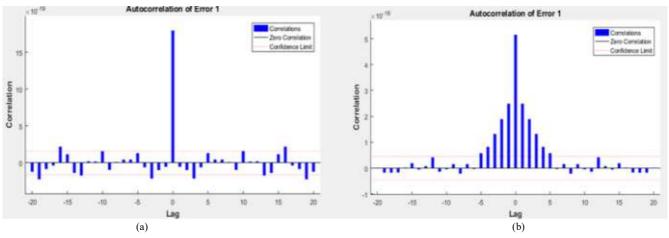
2153

Fig. 10 Auto Correlation: (a) Static Node Environment, (b) Mobile Node Environment

Fig. 10 (a) shows that when the value of time interval (lag) is zero, the correlation value indicated by the blue vertical bar is very high compared to another lag. Therefore, it demonstrates that the correlation of target value to prediction value is very high, which means that the training process for those values is doing well. Fig. 10 (b) shows that when the value of time interval (lag) is zero, the correlation value indicated by the blue vertical bar is very high compared to another lag. There is a correlation value in the lag position of -5 to 5 in certain parts. It means that the correlated data distribution in a static node environment is better than in a mobile node environment. Overall, the correlation of target value to predicted value is very high for both static node and mobile node environments. It is indicated that the training process conceives these two values are doing well.

IV. CONCLUSION

The study proposed a deep learning method for predicting zone radius of ZRP in the next-generation wireless backhaul networks. The problem has been formulated as a time-series prediction problem, and LSTM-RNN as a deep learning variant has been proposed. The proposed approach addresses determining the optimal zone radius for both static and mobile node environments based on various network parameters such as Routing Overhead, Energy Consumption, Throughput, and User Usage. Conventional ZRP is also implemented in obtaining zone radius values to compare with the proposed algorithm.

From the experiment results, 72% of the optimal zone radius value for the proposed algorithm is lower than that of the conventional ZRP in a static node environment. Meanwhile, 54% of the optimal zone radius value for the proposed algorithm in the mobile node environment is lower than that of the conventional ZRP. The proposed LSTM-RNN approaches achieve very small prediction errors for both static and mobile node environments, referring to the mean square error (MSE) value, error distribution histogram, training state, regression, correlation, and time series response. Overall, the correlation of target value to predicted value is very high for both static node and mobile node environments. It is indicated that the training process conceives these two values are doing well. However, the prediction error for the static node

environment is higher than that of the mobile node environment.

The proposed deep LSTM-RNN model for zone radius prediction could be a promising technique. Because it may require adding hardware and/or software, estimating zone radius value could increase the complexity of routing protocols. When the zone radius prediction approach is accurate, the overall performance of the routing protocols can be greatly enhanced. Since we have utilized deep learning models to predict the zone radius value, the computational cost of the training phase is a bit high as it includes forward and backward passes. Future work includes extensions of the current study, such as investigating the network performance using various routing algorithms, Levenberg-Marquardt, and the steepest descent algorithms approach to reach the best performance in zone radius predictions.

REFERENCES

[1] Cisco, "Cisco Annual Internet Report (2018–2023)," *Cisco*, pp. 1–41, 2020, [Online]. Available: http://grs.cisco.com/grsx/cust/grsCustomerSurvey.html?SurveyCode=4153&ad_id=US-BN-SEC-M-CISCOASECURITYRPT-ENT&KeyCode=000112137.

[2] M. Ikram and D. Zhang, "Licensedand UnlicensedSpectrum forFuture 5G/B5G WirelessNetworks," *IEEE Network*, no. August, pp. 6–8, 2019.

[3] A. Alqahtani, R. Abhishek, D. Tipper, and D. Medhi, "Disaster Recovery Power and Communications for Smart Critical Infrastructures," *IEEE Int. Conf. Commun.*, vol. 2018-May, 2018, doi: 10.1109/ICC.2018.8422982.

[4] D. S. Sachin Kumar Gupta, Aabid Rashid Wani, Santosh Kumar, Ashutosh Srivastava, "Wireless Mesh Network Security, Architecture, And Protocols.pdf," in *Security and Privacy Issues In Sensor Networks and IoT*, 2020, pp. 1–27.

[5] A. Barolli, T. Oda, M. Ikeda, L. Barolli, F. Xhafa, and V. Loia, "Node placement for wireless mesh networks: Analysis of WMN-GA system simulation results for different parameters and distributions," *J. Comput. Syst. Sci.*, vol. 81, no. 8, pp. 1496–1507, 2015, doi: 10.1016/j.jcss.2014.12.024.

[6] N. Harrag, A. Refoufi, and A. Harrag, "PSO-IZRP: New enhanced zone routing protocol based on PSO independent zone radius estimation," *Int. J. Numer. Model. Electron. Networks, Devices Fields*, vol. 32, no. 1, pp. 1–16, 2019, doi: 10.1002/jnm.2461.

[7] Y. Fengjie, Y. Hui, and Z. Ying, "Research on DSDV routing protocol based on wireless Mesh network," *Proc. 30th Chinese Control Decis. Conf. CCDC 2018*, pp. 4292–4297, 2018, doi: 10.1109/CCDC.2018.8407870.

[8] A. V. Leonov and G. A. Litvinov, "Applying AODV and OLSR routing protocols to air-to-air scenario in flying ad hoc networks

formed by mini-UAVs," *2018 Syst. Signals Gener. Process. F. Board Commun.*, vol. 2018-Janua, pp. 1–10, 2018, doi: 10.1109/SOSG.2018.8350612.

[9] D. Das, C. R. Tripathy, and M. R. Kabat, "Comparative Study of Proactive and Reactive Routing Protocols in Wireless Grids," *Proc. 3rd Int. Conf. Commun. Electron. Syst. ICCES 2018*, no. Icces, pp. 198–201, 2018, doi: 10.1109/CESYS.2018.8723914.

[10] D. Srivastava, V. Sharma, and D. Soni, "Optimization of CSMA (Carrier Sense Multiple Access) over AODV, DSR WRP Routing Protocol," *Proc. - 2019 4th Int. Conf. Internet Things Smart Innov. Usages, IoT-SIU 2019*, pp. 1–4, 2019, doi: 10.1109/IoT-SIU.2019.8777683.

[11] R. D. G. Sampoornam K P, "Performance Analysis of Bellman Ford, AODV, DSR, ZRP and DYMO Routing Protocol in MANET using EXATA," 2019, doi: 10.1109/ICACCE46606.2019.9079958.

[12] B. Han, L. Ding, Y. Ji, X. Wang, and B. Wang, "A TORA-based Wireless Protocol for MANET with Low Routing Overhead at Link Layer," Dec. 2020, doi: 10.1109/MASS50613.2020.00043.

[13] H. M. Haglan, S. Yussof, K. W. Al-Ani, H. S. Jassim, and D. A. Jasm, "The effect of network size and density to the choice of zone radius in ZRP," *Indones. J. Electr. Eng. Comput. Sci.*, vol. 20, no. 1, pp. 206–213, 2020, doi: 10.11591/ijeecs.v20.i1.pp206-213.

[14] X. Chen, J. Tang, and S. Lao, "Review of Unmanned Aerial Vehicle Swarm Communication Architectures and Routing Protocols," *Appl. Sci.*, vol. 10, no. 10, 2020, doi: 10.3390/app10103661.

[15] R. Gasmi, M. Aliouat, and H. Seba, "A Stable Link Based Zone Routing Protocol (SL - ZRP) for Internet of Vehicles Environment," *Wirel. Pers. Commun.*, no. 0123456789, 2020, doi: 10.1007/s11277-020-07090-y.

[16] M. Kaur and M. Sharma, "Energy Ef fi cient Routing Protocol for MANET," 2018, doi: 10.1007/978-981-10-7386-1.

[17] X. Yang, Q. Chen, C. Chen, and J. Zhao, "Improved ZRP routing protocol based on clustering," *Procedia Comput. Sci.*, vol. 131, pp. 992–1000, 2018, doi: 10.1016/j.procs.2018.04.242.

[18] K. W. Al-ani, S. Yussof, H. M. Haglan, H. Shaker, and L. M. Alani, "Determining an optimum zone radius for zone routing protocol (ZRP) based on node mobility," *Indones. J. Electr. Eng. Comput. Sci.*, vol. 21, no. 2, pp. 1230–1237, 2021, doi: 10.11591/ijeecs.v21.i2.pp1230-1237.

[19] M. Boushaba, A. Hafid, and M. Gendreau, "Node stability-based routing in Wireless Mesh Networks," *J. Netw. Comput. Appl.*, vol. 93, pp. 1–12, 2017, doi: 10.1016/j.jnca.2017.02.010.

[20] F. Tang *et al.*, "On Removing Routing Protocol from Future Wireless Networks: A Real-time Deep Learning Approach for Intelligent Traffic Control," *IEEE Wirel. Commun.*, vol. 25, no. 1, pp. 154–160, 2018, doi: 10.1109/MWC.2017.1700244.

[21] M. Abdel-Nasser, K. Mahmoud, O. A. Omer, M. Lehtonen, and D. Puig, "Link quality prediction in wireless community networks using deep recurrent neural networks," *Alexandria Eng. J.*, vol. 59, no. 5, pp. 3531–3543, 2020, doi: 10.1016/j.aej.2020.05.037.

[22] S. H. S. . Jaffry, "Cellular Traffic Prediction with Recurrent Neural Network," in *2020 IEEE 5th International Symposium on Telecommunication Technologies, ISTT 2020 - Proceedings (pp. 94–98). Institute of Electrical and Electronics Engineers Inc.*, 2020, pp. 94–98, doi: 10.1109/ISTT50966.2020.9279373.

[23] B. Nugraha and R. N. Murthy, "Deep Learning-based Slow DDoS Attack Detection in SDN-based Networks," *2020 IEEE Conf. Netw. Funct. Virtualization Softw. Defin. Networks, NFV-SDN 2020 - Proc.*, pp. 51–56, 2020, doi: 10.1109/NFV-SDN50289.2020.9289894.

[24] L. Mei *et al.*, *Real-time mobile bandwidth prediction using LSTM neural network and Bayesian fusion*, vol. 182. Springer International Publishing, 2020.

[25] C. Petneház, "Recurrent Neural Networks for Time Series Forecasting," *arXiv Prepr. arXiv1901.00069*, no. October, 2019.

[26] Y. B. Razvan Pascanu, Tomas Mikolov, "On the difficulty of training recurrent neural networks Razvan," *Proc. 30th Int. Conf. Mach. Learn. PMLR 28(3)*, vol. 28, no. 3, pp. 1310–1318, 2013, doi: 10.1007/978-3-319-93145-6_3.

[27] P. F. Yoshua Bengio, Patrice Simard, "Learning Long-Term Dependencies with Gradient Descent is Difficult," *IEEE Trans. Neural Networks*, vol. 66, no. 2, pp. 53–61, 1994, doi: 10.1109/72.279181.

[28] J. Sepp Hochreiter and U. Schmidhuber, "Long Short-Term Memory," *Neural Comput.*, vol. 9, pp. 1735–1780, 1997, doi: 10.17582/journal.pjz/2018.50.6.2199.2207.

[29] D. Loghin, S. Cai, G. Chen, T. Tuan, and A. Dinh, "The Disruptions of 5G on Data-Driven Technologies and Applications," *IEEE Trans. Knowl. Data Eng.*, vol. 32, no. 6, pp. 1179–1198, 2020, doi: 10.1109/TKDE.2020.2967670.

[30] T. Yélémou, B. Zerbo, M. T. Dandjinou, and O. Sié, "Impact of ZRP zone radius value on wireless network performance," 2019, doi: 10.1007/978-3-030-16042-5_16.

[31] A. Sharma, Y. D. Lee, and W. Y. Chung, "High accuracy human activity monitoring using neural network," *Proc. - 3rd Int. Conf. Converg. Hybrid Inf. Technol. ICCIT 2008*, vol. 1, pp. 430–435, 2008, doi: 10.1109/ICCIT.2008.394.

[32] Y. Zhang, F. Xiao, F. Qian, and X. Li, "VGM-RNN: HRRP Sequence Extrapolation and Recognition Based on a Novel Optimized RNN," *IEEE Access*, vol. 8, pp. 70071–70081, 2020, doi: 10.1109/ACCESS.2020.2986027.

[33] S. Ruder, "An overview of gradient descent optimization," *arXiv:1609.04747*, pp. 1–14, 2016.

[34] A. Shatnawi, G. Al-Bdour, R. Al-Qurran, and M. Al-Ayyoub, "A comparative study of open source deep learning frameworks," *2018 9th Int. Conf. Inf. Commun. Syst. ICICS 2018*, vol. 2018-Janua, pp. 72–77, 2018, doi: 10.1109/IACS.2018.8355444.

[35] S. Basodi, C. Ji, H. Zhang, and Y. Pan, "Gradient amplification: An efficient way to train deep neural networks," *Big Data Min. Anal.*, vol. 3, no. 3, pp. 196–207, 2020, doi: 10.26599/BDMA.2020.9020004.

[36] R. Pascanu, T. Mikolov, and Y. Bengio, "On the difficulty of training recurrent neural networks," *30th Int. Conf. Mach. Learn. ICML 2013*, no. PART 3, pp. 2347–2355, 2013.

[37] R. Raturi and H. Sargsyan, "A Nonlinear Autoregressive Scheme for Time Series Prediction via Artificial Neural Networks," pp. 14–23, 2018, doi: 10.4236/jcc.2018.69002.

[38] N. Y. Xiao, "Using The Modified Back-propagation Algorithm To Perform Automated Downlink Analysis," Massachusetts Institute Of Technology, 1996.

[39] F. Giannini, V. Laveglia, A. Rossi, D. Zanca, and A. Zugarini, "Neural Networks for Beginners. A fast implementation in Matlab, Torch, TensorFlow," pp. 1–48, 2017, [Online]. Available: http://arxiv.org/abs/1703.05298.

[40] R. A. Gideon, "The correlation coefficients," *J. Mod. Appl. Stat. Methods*, vol. 6, no. 2, pp. 517–529, 2007, doi: 10.22237/jmasm/1193890500.

[41] R. Jos-city, A. Ya, M. L. Abdulrahman, and J. J. Nerat, "LSTM Network for Predicting Medium to Long Term Electricity Usage in Residential Buildings," vol. 9, no. 2, pp. 21–30, 2019, doi: 10.5923/j.computer.20190902.01.